metals

MDPI

Article

Simulation of the Effect of Keyhole Instability on Porosity during the Deep Penetration Laser Welding Process

Yue Kang, Yanqiu Zhao, Yue Li, Jianfeng Wang and Xiaohong Zhan *

College of Materials Science and Technology, Nanjing University of Aeronautics and Astronautics, Nanjing 211106, China; kangyue_nuaa@126.com (Y.K.); zyq_winnie@163.com (Y.Z.); liyue_nuaa@163.com (Y.L.); wangjianfeng@nuaa.edu.cn (J.W.)

* Correspondence: xiaohongzhan_nuaa@126.com; Tel.: +86-151-9585-6181

Abstract: The quality of a laser deep penetration welding joint is closely related to porosity. However, the keyhole stability seriously affects the formation of porosity during the laser welding process. In this paper, a three-dimensional laser welding model with gas/liquid interface evolution characteristics is constructed based on the hydrodynamic interaction between the keyhole and molten pool during the laser welding process. The established model is used to simulate the flow and heat transfer process of molten. The Volume of Fluid (VOF) method is used to study the formation and collapse of the keyhole and the formation of bubbles. It is found that bubbles are easy to form when the keyhole depth abruptly changes. There are three main forms of bubbles formed by keyhole instability. The front wall of the keyhole collapses backward to form a bubble. The back wall of the keyhole inclines forward to form a bubble. The lower part of the keyhole produces a necking-down effect, and the lower part of the keyhole is isolated separately to form a bubble. In addition, when the keyhole does not penetrate the base metal, the stability of the keyhole is high and the percentage of porosity is low.

Keywords: porosity; keyhole instability; VOF; laser welding

check for updates

Citation: Kang, Y.; Zhao, Y.; Li, Y.; Wang, J.; Zhan, X. Simulation of the Effect of Keyhole Instability on Porosity during the Deep Penetration Laser Welding Process. *Metals* **2022**, *12*, 1200. https://doi.org/10.3390/met12071200

Academic Editor: João Pedro Oliveira

Received: 18 June 2022
Accepted: 13 July 2022
Published: 14 July 2022

Publisher's Note: MDPI stays neutral with regard to jurisdictional claims in published maps and institutional affiliations.

Copyright: © 2022 by the authors. Licensee MDPI, Basel, Switzerland. This article is an open access article distributed under the terms and conditions of the Creative Commons Attribution (CC BY) license (https://creativecommons.org/licenses/by/4.0/).

1. Introduction

Laser welding technology has been widely used because of its high efficiency, high welding quality, high precision, good performance, small heat input and small deformation [1–3]. However, the defects of joints, such as porosity and spatter, have been extensively studied by experts. Porosity defects caused by the keyhole in laser welding of Aluminum Alloy are an important defect in laser deep penetration welding [4,5].

During the laser welding process, the driving force of the keyhole wall promotes keyhole formation and maintains keyhole stability. J. Zhou [6–8] carried out force analysis on the keyhole wall, which was affected by the metal vapor recoil pressure and surface tension in the normal direction of the keyhole wall. The shear direction is affected by the Marangoni shear force caused by the surface tension gradient. In a study on the force on the keyhole wall, C.S. Wu and R. Kovacevic [9,10] believe that the force driving the formation of the keyhole is the metal vapor recoil pressure. In addition, the keyhole wall is also affected by the Marangoni shear force caused by the surface tension gradient. The main role of the former is to promote the formation of the keyhole, thus forming deep and narrow weld seams. The main effect of the latter is the formation of Marangoni flow. In the study of the electron beam deep penetration welding mechanism, D. Schauer [11,12] believes that the keyhole wall is affected by the recoil pressure of metal vapor and surface tension by analyzing the force inside the keyhole, and observing that there is a force equilibrium point on the keyhole wall. Under the equilibrium point of force, the metal vapor recoil pressure is greater than the surface tension. Above the equilibrium point of force, the surface tension is greater than the metal vapor recoil pressure. Under the action of the force, the liquid metal

in the upper part of the keyhole flows slightly inward driven by surface tension, reaches the pressure balance area, forms a metal protrusion, and destroys the original pressure balance. After that, the bulge intercepts a part of the incident high-energy beam, so that its temperature increases rapidly, and strong evaporation occurs. The keyhole wall recovers to a smooth state, and the molten pool is further deepened in the process to establish a new pressure balance. Based on the study of keyhole behavior in laser deep penetration welding, H. Wang [13] analyzed the temperature field and molten pool flow field in the laser welding process and studied the influence of keyhole morphology on weld seam formation. The flow state of the molten pool was simulated by analyzing the distribution of keyhole gas pressure. The distribution law of the flow velocity of the liquid metal is obtained, and it is pointed out that the flow velocity decreases at the end of the molten pool. The driving forces of molten pool flow include buoyancy, surface tension, and the force between metal vapor rushing out of the keyhole and the liquid metal.

In the numerical simulation of the high-energy beam welding process, the study of force balance on the keyhole wall and the metal evaporation process is the basis of keyhole morphology and molten pool flow field. The analysis of the front two aspects provides pressure and heat flux boundary conditions for the study of the third aspect from the perspectives of mechanical balance and energy balance.

In this paper, the numerical calculation model of keyhole shape changes and molten pool flow is established, and the transient analysis of keyhole formation and molten pool flow during laser welding is carried out. The relationship between molten pool flow and keyhole stability and porosity defects is established. In the laser welding process, the spontaneous fluctuation and spontaneous perturbation of keyhole depth promote the formation of bubbles. The relationship between bubble formation and keyhole dynamics is studied systematically. The results show that keyhole stability is the main cause of bubble formation. Therefore, this paper is helpful to understand the mechanism of laser deep penetration welding and analyze the causes of porosity defects and put forward the method of weld seam quality control.

2. Materials and Methods

The 6061-T6 Aluminum Alloy used for the test is a 4 mm thick plate. The chemical composition and mechanical properties [14] are shown in Table 1. The welding sample size is 100 × 50 × 4 mm.

Table 1. Chemical compositions of the 6061 Aluminum Alloy and the filler wire (mass fraction, wt.%).

	Si	Mg	Fe	Zn	Cu	Mn	Cr	Ti	Al
6061	0.71	0.94	0.16	0.04	0.19	0.02	0.08	0.03	Bal.
ER4047	5.14	0.05	0.80	0.10	0.30	0.05	-	0.20	Bal.

The leading welding equipment used in the test includes pieces of equipment such as lasers and welding robots, as shown in Figure 1.

The process parameters affecting the laser welding of 6061 Aluminum Alloy include laser power, welding speed, defocusing amount, and shielding gas [15]. In this paper, only the influence of laser power and welding speeds on keyhole morphology and percentage of porosity are discussed. Four sets of tests are conducted here. In the first set of tests, under the determination of small laser power with high welding speed. The second group is obtained under the determination of small laser power with low welding speed. The third group increased the laser power and then used high welding speed. The fourth set of tests was performed under the determination of large laser power with low welding speed. The test process parameters are shown in Table 2.

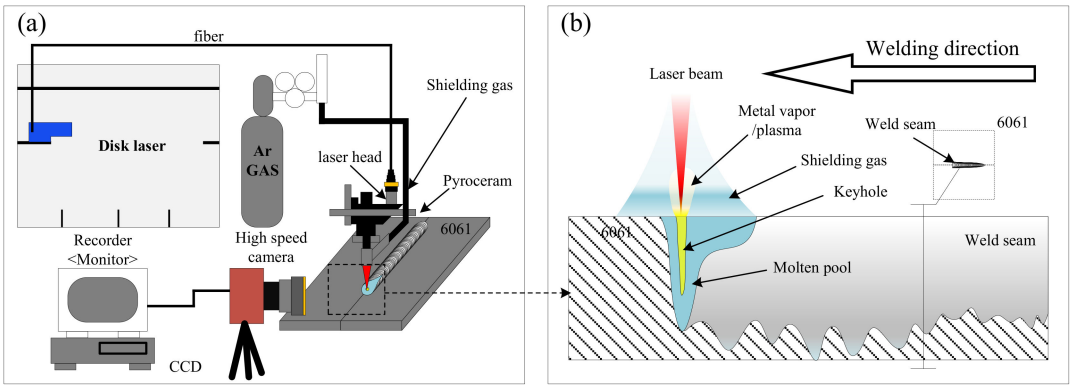

Figure 1. Welding schematic diagram and welding equipment: (**a**) the schematic diagram of the laser welding plate butt joint; (**b**) the schematic diagram of laser deep penetration welding.

Table 2. Welding process parameters.

Process No.	Laser Power (W)	Welding Speed (m/min)	Filler Wire
1	2500	3.0	N
2	2500	2.6	N
3	4500	3.0	N
4	4500	2.6	N

The calculation domain of the model proposed in this paper is shown in Figure 2, including entrance, exit, symmetry plane and wall. The YZ plane is the symmetric plane. The top region of the XY plane is the plasma region. The plane above the plasma region is the entrance, set to a constant speed. Both sides of the plasma region along Y direction and opposite side of symmetry plane are the exits, set to the isobaric surface. The region above the XY plane is the Aluminum Alloy area. The two sides of Aluminum Alloy area along Y directions, opposite side of symmetry plane and bottom are walls.

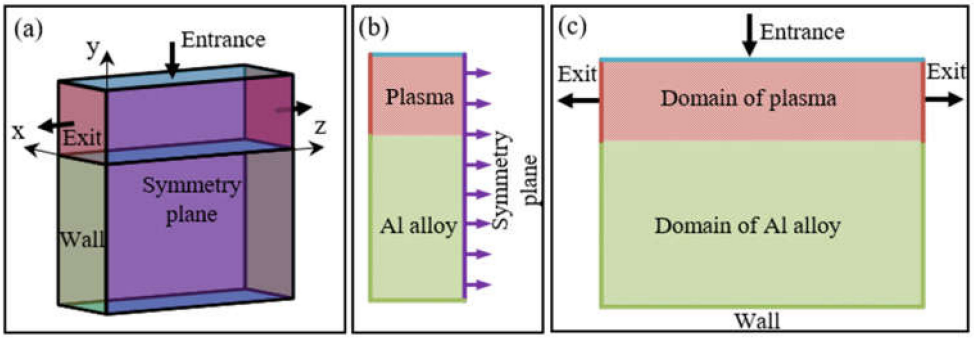

Figure 2. Boundary condition diagram of geometric model: (**a**) three-dimensional diagram; (**b**) cross-section; (**c**) longitudinal section.

Model simplification and assumptions:

1. Assuming that the material is isotropic and the liquid state is incompressible Newtonian fluid in laminar flow mode;

In the laminar boundary layer, the fluid motion is extremely regular. As the velocity increases, the boundary layer exhibits extremely irregular turbulent flow. As a result of the interaction that leads to the chaotic flow state, the velocity and pressure at any point in the turbulent boundary layer fluctuate. The variation of the velocity boundary layer on the plate is shown in Figure 3. In order to simplify the calculation, the liquid flow state is assumed to be laminar.

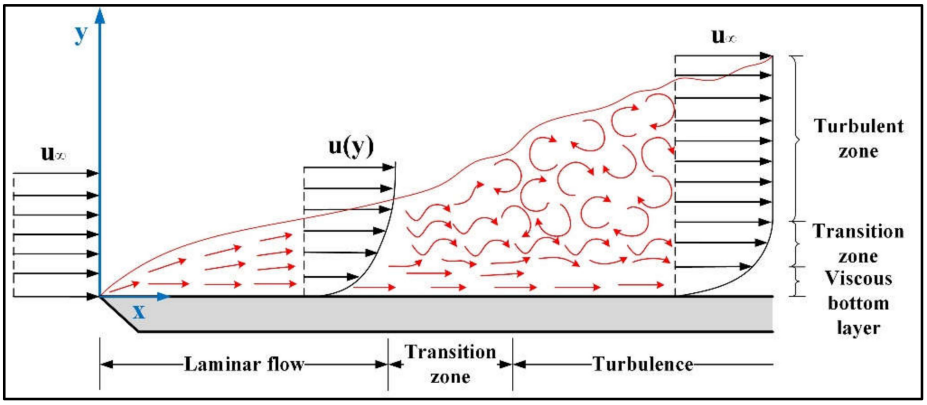

Figure 3. Diagram of Variation of Velocity Boundary Layer on Plate.

2. The liquid region is assumed to be a porous medium with isotropic permeability;
3. Ignoring the effect of shielding gas on molten pool flow and keyhole fluctuation;
4. The shielding effect and absorption effect of the plasma on the laser beam are ignored;
5. The calculation area of molten pool and keyhole is symmetrical about weld seam;
6. The free surface of the molten pool is solved by the Volume of Fluid (VOF) equation. The equation is as follows:

$$\frac{\partial F}{\partial t} + \nabla \cdot (uF) = 0$$

where u is the fluid velocity and F is the volume fraction. In the model established in this paper, the aluminum alloy is the first phase and the plasma is the second phase. When $F = 1$, the control unit is all-aluminum alloy composition.

The specific process of the modeling is shown in Figure 4 below.

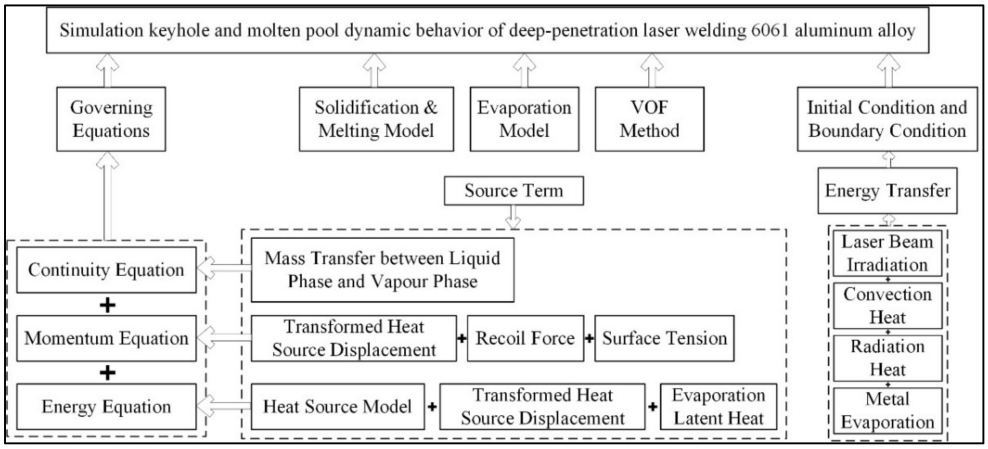

Figure 4. Schematic diagram of numerical model structure.

The basic equations of calculational fluid flow including mass, momentum and energy continuity equations are used to describe the heat transfer, mass transfer and fluid flow in the laser welding process.

The instantaneous time of laser heat source acting on the surface to 6061 Aluminum Alloy is defined as the initial time of calculation.

The molten pool and keyhole will be formed on the surface to be welded from the base metal under the action of the laser beam, which mainly includes the combined action of laser beam irradiation, thermal convection, thermal radiation and metal evaporation.

For the keyhole-free interface in the molten pool, the recoil pressure and surface tension are the main driving forces for the molten pool flow, and they will affect the fluid flow in the molten pool surface area.

In this paper, we only consider the welding process of thermal convection and thermal radiation.

In order to accurately calculate the heating effect of the laser beam on the plate butt structure in the welding process, this paper uses the combined heat source model to simulate the energy transfer of the laser beam in the welding area. The combined heat source model is composed of a Gaussian surface heat source and a Gaussian rotator heat source.

In order to verify the accuracy of the model, the actual process parameters of 6061 Aluminum Alloy plate butt welding are applied to the model for simulation, and the calculation results are compared with the experimental results. For the model verification method, this paper adopts the fusion line contour comparison method for the verification.

In order to fully verify the accuracy of the model, the simulation results under 4 groups of process parameters in the welding test are verified, and the verification results are shown in Figure 5. It can be seen from the figure that the simulation results are in good agreement with the experimental results, although some molten pool and welding seam size parameters present small deviations from the experimental results. In general, the simulation results of the welding seam cross-section profile are basically consistent with the experimental results, and the average error of model accuracy is less than 1%, which indicates that the model used in this paper is more accurate and can be applied to the simulation analysis of 6061 Aluminum Alloy plate butt laser welding process.

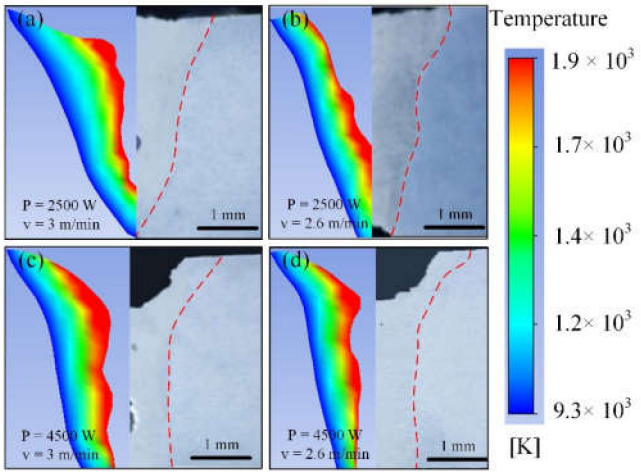

Figure 5. Verification results of thermal-flow coupling model in laser welding process of 6061 Aluminum Alloy plate butt structure: (**a**) P = 2500 W, v = 3 m/min; (**b**) P = 2500 W, v = 2.6 m/min; (**c**) P = 4500 W, v = 3 m/min; (**d**) P = 4500 W, v = 2.6 m/min.

3. Results

3.1. Formation of Keyhole and Molten Pool in Laser Welding Process

It can be seen from Figure 6 that, when the time was 4 ms, the base metal surface was heated and the metal melted. When the time reached 20 ms, the recoil pressure of the molten pool decreased. The recoil pressure here was the lowest, which promoted the formation of a narrow and deep keyhole. As the keyhole depth increased, the surface tension increased, and the surface tension interacted with the recoil pressure to prevent keyhole growth. Finally, the keyhole driving force kept balanced, which made the keyhole maintain a relatively stable state. Before keyhole formation, the laser beam irradiated the base metal surface. When the keyhole was formed, the laser beam was irradiated by metal vapor, and the multiple reflections of the laser beam were realized through the plasma

on the keyhole wall, which improved the efficiency of energy absorption. Therefore, the keyhole became deeper.

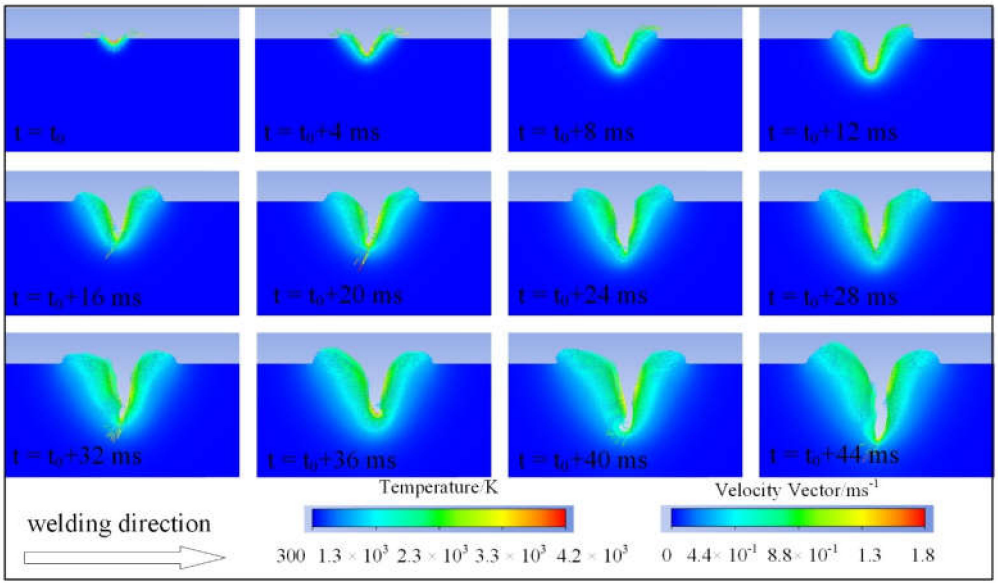

Figure 6. Keyhole formation in laser welding process.

The vector arrow shows the flow trend of the liquid metal in the molten pool. At the top of the keyhole, the liquid metal flowed from the middle of the molten pool to the surrounding entire region, in which the Marangoni flow caused by surface tension absorbed energy from the middle to the surrounding area. Near the keyhole wall, a part of the liquid metal could flow between the surface of the liquid metal and the internal liquid metal due to the temperature gradient and the buoyancy, which played an important role. The other part of the liquid metal flowed along the keyhole surface, and the recoil pressure made the liquid metal flow upward to form a deeper keyhole. However, due to the short welding time and insufficient molten pool length, the Marangoni flow caused by surface tension made the liquid metal flow downward.

3.2. Force Analysis of Keyhole Wall in Laser Welding Process

A point on the keyhole wall is selected for force analysis. The normal upward pressure on the point includes: metal vapor recoil pressure Pg, additional pressure caused by the surface tension of the curved liquid surface Pσ, liquid static pressure caused by gravity Pl, pressure caused by centripetal force considering the rotation of the molten pool Pc, and the laser beam impact force, which can be ignored. Shear force in the tangent direction includes shear force caused by tangential velocity F_s and shear force caused by surface tension gradient Fσ, as follows in Figure 7.

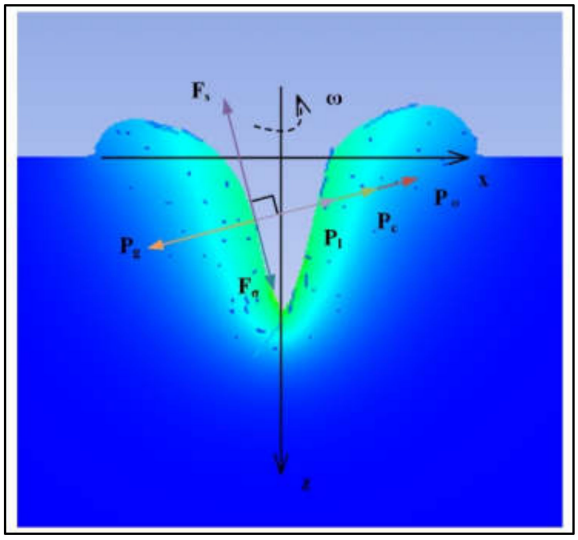

Figure 7. Force analysis of keyhole wall.

In the laser welding process, the direction from the liquid phase to the gas phase is specified as the positive direction. When the keyhole reaches the dynamic balance state, the normal direction resultant force on the keyhole wall is zero.

$$P_g(r) = ABexp\left(-\frac{\triangle_{vap}H_m}{R}\cdot\frac{1}{T(r)}\right) \quad (1)$$

where A is a coefficient related to the surrounding environment, A = 1 at atmospheric pressure [16]; B is a coefficient associated with the integral constant, and the value of parameter B is determined by referring to the saturated vapor pressure of pure Aluminum at 2740 K under a standard state, $B = 3.55 \times 10^{10}$; $T(r)$ means the temperature distribution in the free surface.

$$P_\sigma = 2\sigma H \quad (2)$$

$$P_\sigma = \sigma\cdot(1/r_1 + 1/r_2) \quad (3)$$

In the Young–Laplace equation, $r1$ and $r2$ refer to the maximum and minimum curvature radius of the surface, respectively, and $\frac{1}{2}\cdot(1/r1 + 1/r2)$ refers to the degree of curvature at any point of the surface.

$$P_l = \rho g z \quad (4)$$

$$P_c = \frac{\rho\omega^2 r^2}{2} \quad (5)$$

Considering the rotation of the molten pool, the pressure distribution caused by centripetal force is solved according to the law of statics. When the centripetal force is volumetric force, the centripetal force of unit mass at the radius r on the keyhole wall is $r\omega^2$.

With the decrease of keyhole wall radius, namely the increase of keyhole depth, the liquid static pressure increases, the rotational centripetal force of the molten pool decreases, the metal vapor recoil pressure increases and the additional pressure that is caused by surface tension increases. The metal vapor recoil pressure and additional pressure are much larger than the static pressure and centripetal force. The main force to maintain the dynamic balance of the keyhole is the additional pressure caused by the metal vapor recoil pressure and surface tension. The metal vapor recoil pressure promotes the formation of the keyhole and maintains the stability of keyhole morphology. The additional pressure caused by surface tension inhibits keyhole formation.

In the upper half part of the keyhole, the curvature of the keyhole wall is relatively uniform, so that the additional pressure caused by surface tension is evenly distributed. In addition, the small temperature gradient on the keyhole wall also causes the distribution

of additional pressure caused by surface tension uniform. At the same time, the distribution of metal vapor recoil pressure tends to be uniform.

In the lower part of the keyhole, the curvature of the keyhole wall is large, and the additional pressure caused by surface tension increases rapidly with the increase of the depth of the keyhole. Concomitantly, in order to maintain the stability of keyhole morphology, the metal vapor recoil pressure needs to be increased rapidly to offset the effect of surface tension.

3.3. Influence of Process Parameters on Dynamic Behaviour of Keyhole and Bubble Formation

The effects of laser power and welding speed on keyhole morphology were discussed. The keyhole depth, width, area, front wall inclination angle of the keyhole and back wall inclination angle of the keyhole were measured at different times, as shown in Figure 8. For any measured values for each group of test parameters, 80 consecutive simulation results were analyzed.

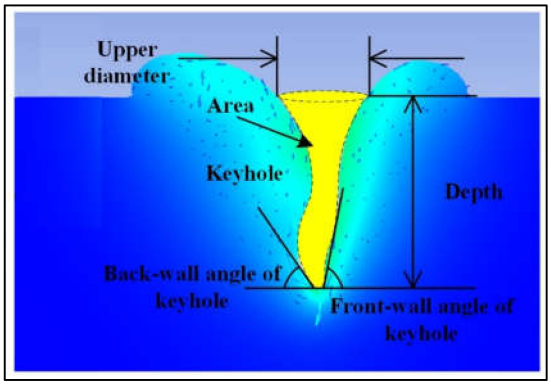

Figure 8. Illustration of keyhole shape with depth, outlet diameter of keyhole top, area of keyhole, front wall inclination angle of keyhole, and back wall inclination angle of keyhole.

In the molten pool, a keyhole with dense plasma metal vapor can be regarded as a cavity. The filling mode of the liquid metal determines whether bubbles are formed during the laser welding process. The backfill method of liquid metal mainly has two forms. One is that the front wall of the keyhole bulges and collapses backward. The other is the keyhole back wall bulges and collapses forward. Another way is that the necking-down phenomenon occurs at the neck of the keyhole, and the lower part of the keyhole is separated to form a separate bubble.

In this paper, the keyhole depth and the outlet diameter at the top of the keyhole under different process parameters are analyzed, and the following regulations are found, as shown in Figures 9 and 10.

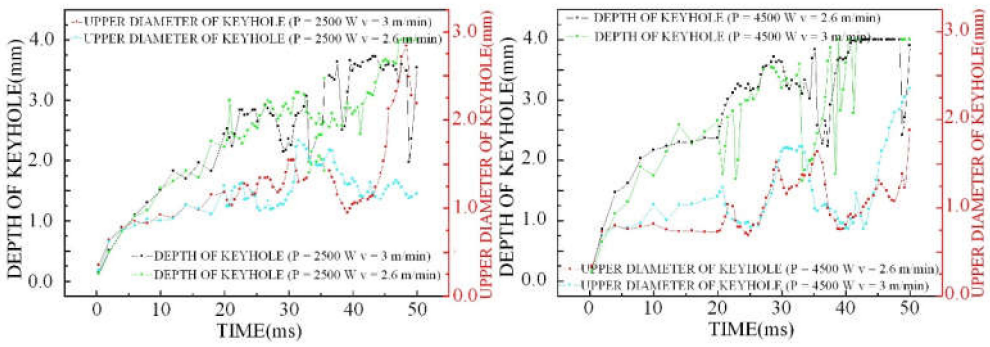

Figure 9. Effect of welding speed on keyhole depth and outlet diameter of keyhole top.

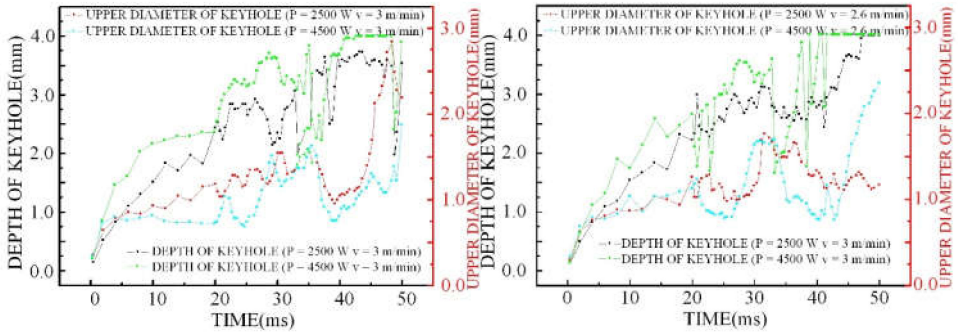

Figure 10. Effect of laser power on keyhole depth and outlet diameter of keyhole top.

When laser power is insufficient to form a keyhole through the base metal, the keyhole depth increases with the decrease in welding speed. When laser power is large enough to form a keyhole through the base metal, the keyhole depth is equal to the thickness of the base metal. When welding speed is high, the increase in the outlet diameter size of the keyhole top is more significant than that at low welding speed.

Comparing different laser powers, it was found that when the laser power is large, excessive heat input leads to a large fluctuation of keyhole depth. Moreover, when the heat input is large, the effect of increasing the outlet diameter of the keyhole top is more significant than that of small heat input.

In addition, through the statistics of the keyhole depth and the outlet diameter of the keyhole top under different process parameters, it was found that bubbles were easily formed when the keyhole depth changed, as shown in Figure 11, along with the outlet diameter size of the keyhole top fluctuations.

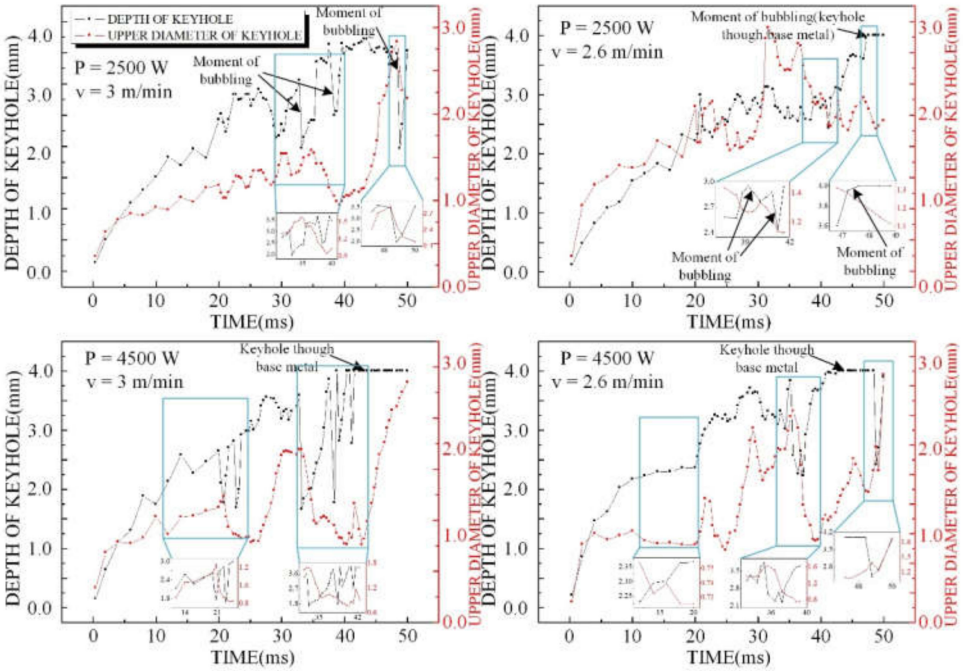

Figure 11. Effect of process parameters on keyhole instability.

Bubble formation induced by the keyhole leads to rapid instability of keyhole and changes in the keyhole depth. Therefore, the formation of bubbles can be judged according to the change of keyhole in the laser welding process, which provides help for the detection of porosity defects in the laser welding process.

In the laser welding process, due to the interaction between different dynamic mechanisms in the molten pool, the keyhole is unstable and the keyhole profile fluctuates over

time. Inside the keyhole, the convergence of the liquid metal leads to a bulge and collapse of the keyhole wall. As shown in Figure 12, according to the simulation results, the keyhole profile at different times during the laser welding process is extracted, and bubbles formed by the keyhole collapse are counted. The porosities formed by the keyhole are closely related to bubbles. The variation trend of bubble formation in keyholes under different process parameters was quantitatively compared.

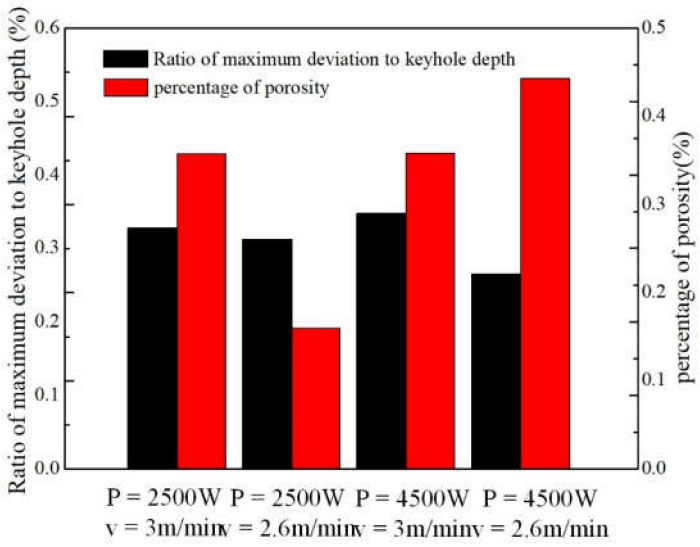

Figure 12. Effect of process parameters on ratio of maximum deviation to keyhole depth and percentage of porosity.

In order to evaluate the stability of a keyhole, this paper determines the maximum deviation of the keyhole depth relative to the average keyhole depth. The ratio of maximum deviation to keyhole depth is expressed as follows [17]:

$$\sigma = \frac{d}{D} \times 100 \tag{6}$$

where σ is the ratio of maximum deviation to keyhole depth; d is the maximum deviation depth of the keyhole; and D is the average keyhole depth.

The percentage of porosity, R_p, is defined as the sum of porosity diameters per unit of weld seam length in the welding direction [4].

$$R_p = \frac{L_p}{L_w} \times 100\% \tag{7}$$

where L_w is the weld seam length and L_p is the sum of porosity diameters in the welding direction.

According to Figure 11, by comparing the ratio of maximum deviation to the keyhole depth, it is concluded that the keyhole is relatively stable when the laser power is low. When the laser power is high, reducing the welding speed can make the keyhole relatively stable. When the laser power is high, the keyhole is relatively stable. However, the percentage of porosity is increased because the keyhole runs through the base metal leading the bottom of the keyhole to contact with the air and to enter the air. Therefore, the percentage of porosity is low when the keyhole stability is high.

Figure 13 shows the influence of process parameters on the keyhole area, the front wall inclination angle of the keyhole and the back wall inclination angle of the keyhole.

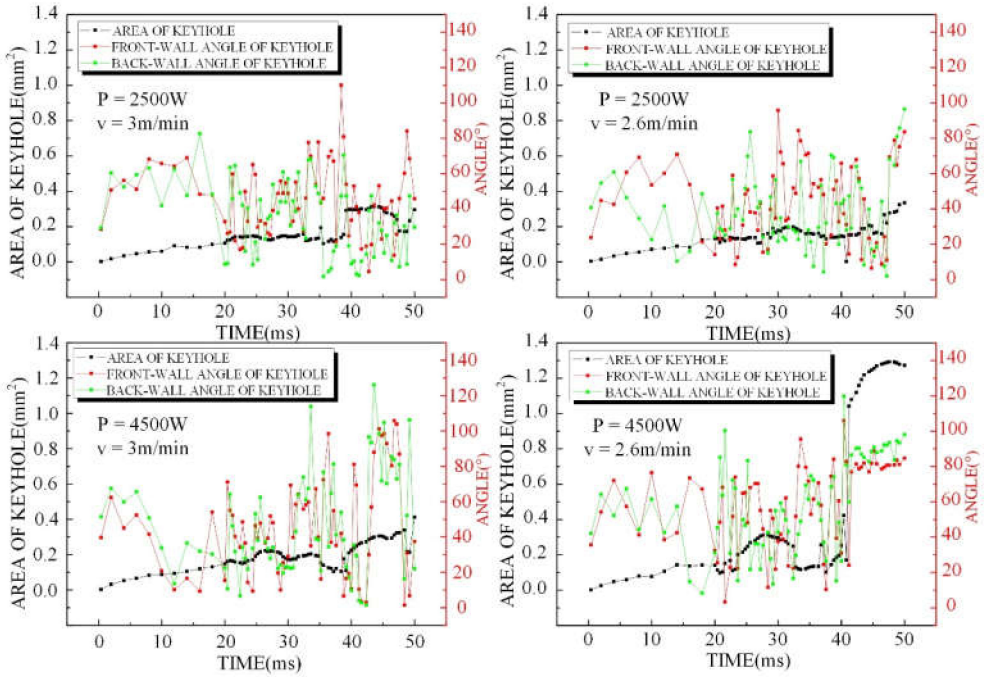

Figure 13. Effect of process parameter on area of keyhole, front wall angle of keyhole, and back wall angle of keyhole.

Through horizontal comparison, the relationship between the keyhole area, front wall inclination angle and back wall inclination angle of the keyhole is studied under different welding speeds and it is researched through longitudinal comparison under different laser powers. It was found that when the laser power is too high, the keyhole is formed through the base metal, and the keyhole area increases sharply. The front wall inclination angle and the back wall inclination angle of the keyhole through the base metal are relatively stable. When the laser power is low, the front wall inclination angle and back wall inclination angle of the keyhole are relatively stable.

3.4. Relationship between Dynamic Behaviour of Keyhole and Bubble Forming

The tip at bottom of the keyhole tilts backward, the lower half part of the liquid metal on the back wall of the keyhole flows clockwise, and the upper half part flows counterclockwise. The middle position of the molten pool behind the keyhole intersects and forms a bulge, which finally leads to the collapse of the keyhole and forms a bubble below the keyhole. If bubbles cannot escape from the molten pool due to the flow behavior of the liquid metal, porosities will eventually form [18].

In this paper, it was found that there are two main reasons for a 'bulge'. One is a sudden change in the temperature at a certain position of the keyhole wall, resulting in a mutation in metal vapor recoil pressure, resulting in the emergence of bulges. The other is the abrupt change of curvature at a certain position of the keyhole wall, which leads to the mutation of surface tension and thus induces a bulge.

During laser welding, a bulge on the keyhole wall makes laser radiation and gas pressure at the bottom of the keyhole decrease rapidly. Simultaneously, a low-pressure zone appears near the keyhole outlet when extremely high-speed metal vapor is ejected from the outlet at the top of the keyhole. Low pressure will make the keyhole absorb the surrounding gas. As a result, ambient gases enter the keyhole.

In the laser welding molten pool, a keyhole with dense plasma metal vapor can be regarded as a cavity. The filling mode of the liquid metal determines whether bubbles are formed during the welding process. There are three forms of liquid metal backfill. One is that the keyhole back wall bulge causes a collapse forward. The other is the front wall of the keyhole bulges and collapses backward. Another way is that necking-down occurs

in the lower part of the keyhole, and separate bubbles are formed in the lower part of the keyhole.

During the laser welding process, the tip of the keyhole's lower part inclines forward when the keyhole is stable. Before keyhole instability, the tip of the keyhole bottom inclines, as shown in Figure 14.

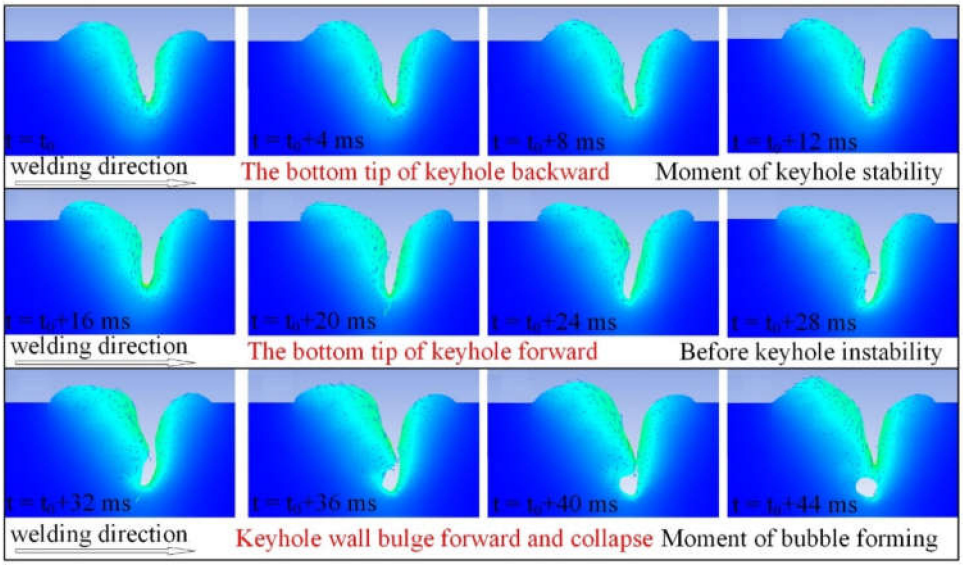

Figure 14. Bubble formation process caused by bulge and collapse of keyhole back wall.

The metal vapor pressure continues under the cation of the laser beam for a period of time. At the same time, the keyhole plasma concentrates the heat source energy in the keyhole region, which increases the temperature gradient near the top outlet of the keyhole. Inside the molten pool in the upper half of the keyhole, the shear stress of the Marangoni and vapor pressure force the liquid metal to resist the gravity flow out of the top outlet of the keyhole. This is a resistance to liquid metal collapse from the top of the keyhole. However, in the deep region of the keyhole, Marangoni shear stress and metal vapor pressure are weak in the lower half. Therefore, the gravity effect is generated and stable liquid metal backfill is carried out [19].

The tip of the bottom keyhole leans forward leading to the collapse of the front wall of the keyhole forming a bubble, as shown in Figure 15.

In the laser welding process, the front wall of the keyhole is slightly bent backward, and a bulge is generated in the part where the local bending degree of the front wall changes slightly. The liquid metal near the bulge evaporates violently under the high-energy irradiation of the laser beam. The vaporized metal vapor is ejected at a large speed on the back wall from the concave and if impacted by the metal vapor flow, is a liability to fall and collapse under the action of complex physical conditions such as gravity. As a result, the keyhole collapses and closes, eventually forming bubbles [8].

In the laser welding process, various driving forces in the molten pool interact with each other, and the keyhole is in an unstable state with intense oscillation. At the time of t0, the keyhole begins to shrink, the diameter of the keyhole's middle part becomes smaller, and the front wall and back wall of the keyhole's middle part bulges, as shown in Figure 16. The liquid metal intersection at the neck of the keyhole makes the keyhole shrink, and the cavity at the bottom of the keyhole is blocked at the bottom of the molten pool.

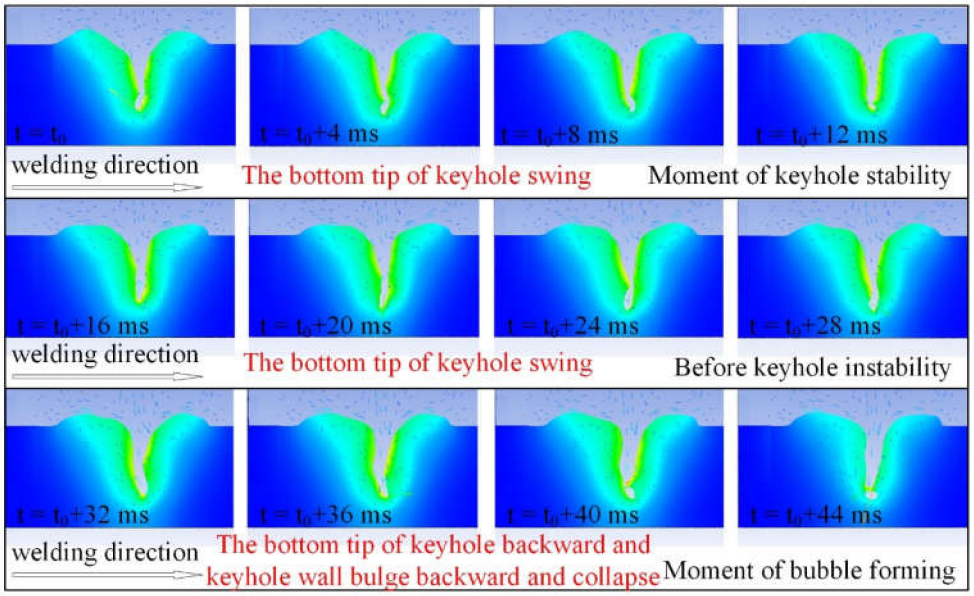

Figure 15. Bubble formation process caused by bulge and collapse of keyhole front wall.

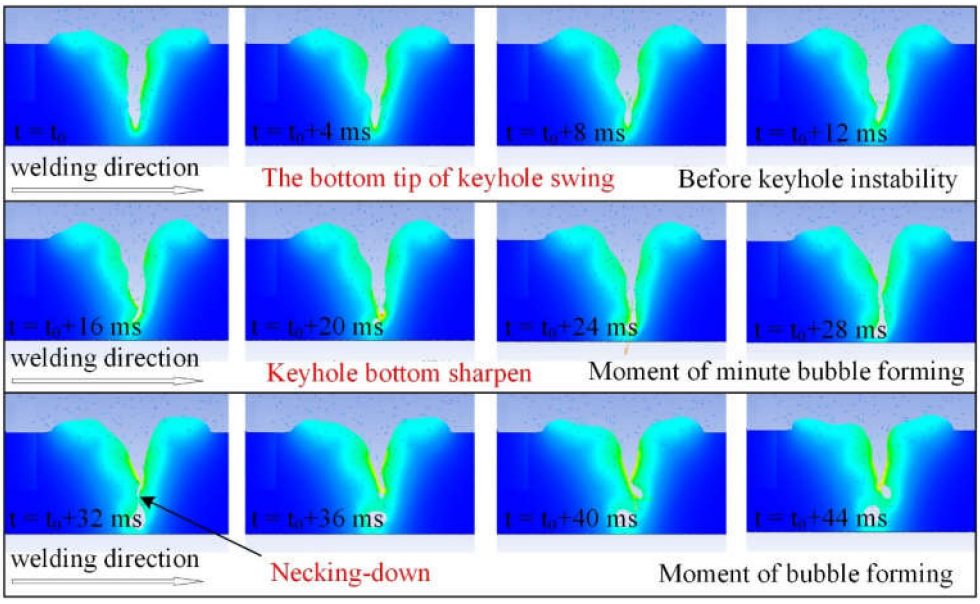

Figure 16. Bubble formation process caused by necking-down of keyhole.

In the molten pool, there is a liquid metal flowing downward, and there is also a liquid metal flowing upward. Their encounter leads to the bulge of the keyhole wall. The keyhole wall collapses and bubbles form at the bottom of the molten pool, which suddenly reduces the keyhole depth. Liquid metal flow in the molten pool makes bubbles shrink and become trapped in the molten pool. At the top of the molten pool, liquid metal flows from the center to around the sides. At the bottom of the molten pool, there are two opposite flows. One flows from the top to the middle. One flows from the bottom to the middle. Due to the existence of two opposite flow directions, the surface of the keyhole wall is bulged, resulting in the collapse and contraction of the keyhole.

According to the stability theory of capillarity, when the height of capillarity is greater than the circumference of its cross-section, the capillarity would be in an unstable state, and the necking-down and expansion would alternate. Especially, there is a trend of shrinkage and closure at the necking-down stage. Corresponding to the actual laser welding process, the keyhole is in this state. When the energy density of the laser beam is higher than a

critical value, the recoil pressure generated by the metal vapor would expand the degree of necking down. At the same time, the necking-down collapse trend of liquid metal around the keyhole interacts with the metal vapor recoil pressure, making the keyhole vibrate back and forth in the radial direction. When the laser beam energy density at the bottom of the keyhole is lower than the critical value for maintaining the keyhole stability due to the absorption of laser energy by the plasma in the keyhole or other factors, the keyhole would be closed at the necking-down stage to form a bubble.

4. Conclusions

A three-dimensional thermal-fluid coupling model was established for the laser welding of a 4 mm thick 6061 Aluminum Alloy plate butt structure. The driving force of the keyhole during the laser welding process was analyzed and added to the model to simulate the dynamic of the keyhole under different process parameters. The conclusions drawn from the present study are given below.

(1) When P = 2500 W, v = 3 m/min, is the critical value of weld penetration. The formation of a bubble is usually caused by the driving force of the molten pool and keyhole surface during laser deep penetration welding. The main reason for the formation of keyhole porosity is the instability of the keyhole.
(2) In the laser welding process, the keyhole is unstable due to the interaction of different driving forces, and the keyhole contour fluctuates over time. The liquid metal flow at the keyhole wall leads to a bulge, which eventually leads to the collapse of the keyhole wall.
(3) During the laser welding process, the spontaneous fluctuation of keyhole depth and the spontaneous disturbance of the keyhole promote the formation of bubbles.
(4) The three types of bubble formation caused by keyhole dynamic behavior are: The tip of the keyhole bottom leans forward, and the back wall of the keyhole collapses, forming bubbles behind the keyhole; The tip of the keyhole bottom leans backward, and the front wall of the keyhole collapses, forming bubbles in front of the keyhole. A sharp shrinkage fracture occurs in the middle of the keyhole, forming bubbles below the keyhole.

Author Contributions: Conceptualization, Y.K.; data curation, Y.Z.; formal analysis, Y.L.; investigation, J.W.; resources, X.Z. All authors have read and agreed to the published version of the manuscript.

Funding: The authors gratefully acknowledge the financial support of the project from the Fundamental Research Funds for the Central Universities (Grant No. NS2022062), the Fundamental Research Funds for the Central Universities (Grant No. NS2021045), and the Scientific Research Foundation for Introduced Talents of Nanjing University of Aeronautics and Astronautics.

Institutional Review Board Statement: Not applicable.

Informed Consent Statement: Not applicable.

Data Availability Statement: Data available on request due to restrictions, e.g., privacy or ethics. The data presented in this study are available on request from the corresponding author. The data are not publicly available due to privacy.

Conflicts of Interest: The authors declare no conflict of interest.

References

1. Jin, Y.; Oliveira, J.P.; Yulong, L.; Caiwang, T.; Chenkai, G.; Yixuan, Z.; Zhishui, Y. Laser techniques for dissimilar joining of aluminum alloys to steels: A critical review. *J. Mater. Process. Technol.* **2022**, *301*, 117443.
2. Oliveira, J.P.; Jiajia, S.; Escobar, J.D.; Salvador, C.A.F.; Schell, N.; Zhou, N.; Benafan, O. Laser welding of H-phase strengthened Ni-rich NiTi-20Zr high-temperature shape memory alloy. *Mater. Des.* **2021**, *202*, 109533. [CrossRef]
3. Oliveira, J.P.; Shamsolhodaei, A.; Jiajia, S.; Lopes, J.G.; Goncalves, R.M.; Mariana, B.F.; Loirenco, P.; Zeng, Z.; Schell, N.; Zhou, N.; et al. Improving the ductility in laser welded joints of CoCrFeMnNi high entropy alloy to 316 stainless steel. *Mater. Des.* **2022**, *219*, 110717. [CrossRef]

4. Zhao, H.; He, L.; Niu, W.C.; Zhang, B. Investigation on porosity suppression in deep-penetration laser welding by using computational fluid dynamics. *J. Laser Appl.* **2016**, *28*, 032011. [CrossRef]
5. Cao, X.; Wallace, W.; Poon, C.; Immarigeon, J.P. Research and progress in laser welding of wrought aluminum alloys. II. metallurgical microstructures, defects, and mechanical properties. *Adv. Manuf. Process.* **2003**, *18*, 23–49. [CrossRef]
6. Zhou, J.; Tsai, H.L. Effects of electromagnetic force on melt flow and porosity prevention in pulsed laser keyhole welding. *Int. J. Heat Mass Transf.* **2007**, *50*, 2217–2235. [CrossRef]
7. Zhou, J.; Lung, H.T.; Wang, P.C. Transport phenomena and keyhole dynamics during pulsed laser welding. *J. Heat Transf.* **2006**, *128*, 680–690. [CrossRef]
8. Zhou, J.; Lung, H.T. Porosity formation and prevention in pulsed laser welding. *J. Heat Transf.* **2007**, *129*, 1014–1024. [CrossRef]
9. Fan, H.G.; Kovacevic, R. A unified model of transport phenomena in gas metal arc welding including electrode, arc plasma and molten pool. *J. Phys. D Appl. Phys.* **2004**, *37*, 2531. [CrossRef]
10. Wu, C.S.; Sun, J.S.; Zhang, Y.M. Numerical simulation of dynamic development of keyhole in double-side arc welding. *Model. Simul. Mater. Sci. Eng.* **2004**, *12*, 423. [CrossRef]
11. Schauer, D.A. Thermal and Dynamic Effects in Electron Beam Welding Cavities. Ph.D. Thesis, University of California Livermore, Livermore, CA, USA, 1977.
12. Schauer, D.A.; Geidt, W.H. Prediction of electron beam welding spiking tendency. *Weld. Res. Suppl.* **1978**, *57*, 189–195.
13. Hong, W.; Shi, Y.; Gong, S. Effect of pressure gradient driven convection in the molten pool during the deep penetration laser welding. *J. Mater. Process. Technol.* **2007**, *184*, 386–392.
14. Zhan, X.; Chen, J.; Liu, J.; Wei, Y.; Zhou, J.; Meng, Y. Microstructure and magnesium burning loss behavior of AA6061 electron beam welding joints. *Mater. Des.* **2016**, *99*, 449–458. [CrossRef]
15. Ahn, J.; Chen, L.; Davies, C.M.; Dear, J.P. Parametric optimisation and microstructural analysis on high power Yb-fibre laser welding of Ti-6Al-4V. *Opt. Lasers Eng.* **2016**, *86*, 156–171. [CrossRef]
16. Semak, V.; Matsunawa, A. The role of recoil pressure in energy balance during laser materials processing. *J. Phys. D Appl. Phys.* **1977**, *30*, 2541.
17. Miyagi, M.; Wang, J. Keyhole dynamics and morphology visualized by in-situ X-ray imaging in laser melting of austenitic stainless steel. *J. Mater. Process. Technol.* **2020**, *282*, 116673. [CrossRef]
18. Chen, M.; Xu, J.; Xin, L.; Zhao, Z.; Wu, F.; Ma, S.; Zhang, Y. Effect of keyhole characteristics on porosity formation during pulsed laser GTA hybrid welding of AZ31B magnesium alloy. *Opt. Lasers Eng.* **2017**, *93*, 139–145. [CrossRef]
19. Zhao, H.; Niu, W.; Zhang, B.; Lei, Y.; Kodama, M.; Ishide, T. Modelling of keyhole dynamics and porosity formation considering the adaptive keyhole shape and three-phase coupling during deep-penetration laser welding. *J. Phys. D Appl. Phys.* **2011**, *44*, 486302. [CrossRef]